References and Notes

1. G. H. Pettengill and R. B. Dyce, *Nature* (*Lond.*) **206**, 1240 (1965).
2. G. Columbo, *ibid.* **208**, 575 (1965); P. Goldreich and S. Peale, *Astron. J.* **71**, 425 (1966); G. Columbo and I. I. Shapiro, *Astrophys. J.* **145**, 296 (1966).
3. G. P. Kuiper, *Commun. Lunar Planet. Lab.* **143**, 165 (1970).
4. S. J. Peale, *Icarus* **17**, 168 (1972); *Astron. J.*, in press.
5. G. Field, in *The Origin and Evolution of the Atmospheres and Oceans*, P. J. Brancazio and A. G. W. Cameron, Eds. (Wiley, New York, 1964).
6. S. I. Rasool, S. H. Gross, W. E. McGovern, *Space Sci. Rev.* **5**, 565 (1966).
7. D. Morrison and C. Sagan, *Astrophys. J.* **150**, 1105 (1967); D. Morrison, *Space Sci. Rev.* **11**, 271 (1970).
8. W. Elsasser, *Phys. Rev.* **9**, 106 (1946); E. C. Bullard and H. Gellman, *Philos. Trans. R. Soc. Lond. Ser. A Math. Phys. Sci.* **247**, 213 (1954); W. V. R. Malkus, *Science* **160**, 259 (1968); D. Gubbins, *Rev. Geophys. Space Phys.* **12**, 137 (1974).
9. N. F. Ness and Y. C. Whang, *J. Geophys. Res.* **76**, 3136 (1971).
10. P. M. Banks, H. E. Johnson, W. I. Axford, *Comments Astrophys. Space Phys.* **2**, 214 (1970).
11. C. P. Sonett and D. S. Colburn, *Phys. Earth Planet. Interiors* **1**, 326 (1968); J. L. Blank and W. Sill, *J. Geophys. Res.* **74**, 736 (1969); G. Schubert and K. Schwartz, *Moon* **1**, 106 (1969).
12. N. F. Ness, K. W. Behannon, R. P. Lepping, Y. C. Whang, K. H. Schatten, *Science* **183**, 1301 (1974).
13. E. W. Greenstadt, I. M. Green, G. T. Inouye, D. S. Colburn, J. H. Binsack, E. F. Lyon, *Cosmic Electrodyn.* **1**, 160, 279, and 316 (1970); E. W. Greenstadt, *J. Geophys. Res.* **77**, 1729 and 5467 (1972); T. G. Northrop and T. J. Birmingham, *ibid.* **78**, 2308 (1973).
14. J. Y. Choe, D. B. Beard, E. C. Sullivan, *Planet. Space Sci.* **21**, 485 (1973).
15. A. W. Rizzi, thesis, Stanford University (1971).
16. D. C. Colburn and C. P. Sonett, *Space Sci. Rev.* **5**, 439 (1966).
17. J. K. Chao, *MIT Report CSR TR-70-3* (1970); R. P. Lepping and P. D. Argentiero, *J. Geophys. Res.* **76**, 4349 (1971).
18. L. F. Burlaga and K. W. Oglivie, *Astrophys. J.* **159**, 659 (1970).
19. G. R. Smit, *ESRO Report SN-17* (European Space Research Institute, Frascati, Italy, 1967); B. Bavassano, F. Mariani, U. Villante, N. F. Ness, *J. Geophys. Res.* **76**, 5970 (1971); *ibid.* **77**, 2004 (1972).
20. L. F. Burlaga and N. F. Ness, *Solar Phys.* **9**, 467 (1969); D. M. Willis, *Rev. Geophys. Space Phys.* **9**, 953 (1971).
21. S. Chapman and J. Bartels, *Geomagnetism* (Clarendon, Oxford, 1940).
22. S. Plagemann, *J. Geophys. Res.* **70**, 985 (1965); R. A. Lyttleton, *Astrophys. Space Sci.* **5**, 18 (1969).
23. D. S. Colburn, C. P. Sonett, K. Schwartz, *Earth Planet. Sci. Lett.* **14**, 325 (1972).
24. A. J. Dessler, in *Atmospheres of Venus and Mars*, J. C. Brandt and M. B. McElroy, Eds. (Gordon & Breach, New York, 1968), p. 241; F. S. Johnson and J. E. Midgeley, *Space Res.* **9**, 760 (1969); F. C. Michel, *Rev. Geophys. Space Sci.* **9**, 427 (1971); J. L. Blank and W. R. Sill, *Bellcomm. TM 72-2015-1* (1972); P. A. Cloutier and R. E. Daniell, *Planet. Space Sci.* **21**, 463 (1973).
25. G. Schubert, and B. Horning, in preparation.

26. We appreciate discussions of these results with our colleagues from the plasma science experiment and charged particle experiment teams. In addition, our colleagues at Goddard, D. Howell, H. Burdick, R. Hoffman, J. Seek, and J. Scheifele, contributed significantly in the phases of the mission concerned with the magnetometer boom, instrumentation, and data analysis. Lastly, we recognize the contributions of the technical teams at Jet Propulsion Laboratory and the Boeing Company to the successful conduct of the overall mission; we especially acknowledge J. Bruns of Boeing in connection with this experiment.

29 May 1974

Electrons and Protons Accelerated in Mercury's Magnetic Field

Abstract. *Fluxes of protons with energies of* ~ 550 *kev and electrons with energies of* ~ 300 *kev which exceed approximately* 10^4 *and* 10^5 cm^{-2} sec^{-1}, *respectively, have been discovered in the magnetosphere of Mercury. Electron fluxes* $> 10^3$ cm^{-2} sec^{-1} *also are observed in the outbound pass of the Mariner 10 spacecraft through the magnetosheath. The intensity versus time profiles of the particle fluxes in the magnetosphere appear with sudden onsets of* $\sim 10^4$ cm^{-2} sec^{-1} *beginning at interplanetary background levels and persisting for times equivalent to their being distributed spatially over regions having a scale size comparable to the planetary radius. For a spectral form* $dJ/dE \propto E^{-\gamma}$, *where* J *is the differential particle intensity and* E *is the kinetic energy, the typical values of* γ *are* $\gamma_p = 5.5$ *for protons above 500 kev and* $\gamma_e \geqq 9$ *for electrons above 170 kev. Large coherent electron intensity oscillations (variations of factors of 10 to 100) have been discovered with characteristic periods of* ~ 6 *seconds and with higher frequency components. In some cases proton bursts are found in phase with these oscillations. On the basis of the experimental evidence and a knowledge of the general magnetic field intensities and directions along the trajectory of Mariner 10 provided by the magnetic field observations, it is shown that the radiation events observed in the magnetosphere and magnetosheath are transient and are not interpretable in terms of stable trapped particle populations. Furthermore, experimental evidence strongly supports the view that the particles are impulsively accelerated and that the acceleration source is not more distant from the point of observation along lines of force than* $\sim 8 \times 10^3$ *to* 16×10^3 *kilometers (3 to 6.5 units of Mercury's radius). Candidates for the regions most likely to be sources of particle acceleration are discussed, namely, the magnetotail and the magnetosheath. It is pointed out that the phenomena discovered at Mercury will place more stringent conditions on allowed models for electron and proton acceleration than have heretofore been possible in studies within the earth's magnetosphere.*

One of the outstanding problems of common interest for planetary electrodynamics and high energy astrophysics is the acceleration of electrons and protons arising from the solar wind interaction with the induced or intrinsic magnetic fields of the planets. A wide range of in situ measurements already made at four planets and at the moon serve as a basis for an investigation of the physical conditions necessary for particle acceleration. Only at the earth and Jupiter, which have intrinsic magnetic fields with extensive magnetospheres, has local acceleration been shown to exist for both trapped radiation and impulsive events of electrons and protons. For Venus and Mars, without intrinsic magnetic fields but with ionospheres which provide a conducting surface for the interaction with the solar wind, induced magnetic fields are generated and standoff bow shocks have been observed. No evidence has been found for particle acceleration above an energy of ~ 50 kev in either the bow shock or the plasma wake region of either Venus or Mars. The moon represents the extreme case of a solid body without appreciable intrinsic magnetic field, ionosphere, or any conducting surface to deflect the solar wind. It has neither a bow shock nor significant induced magnetic fields which could lead to charged particle acceleration. Therefore, in attempts to predict the conditions for particle acceleration at Mercury the evidence derived from these earlier studies suggested that unless Mercury had a significant intrinsic magnetic field (*1*, *2*), which was believed doubtful on the basis of its slow rotational period (*3*), the planet would most likely have a moonlike interaction with the solar wind (*1*, *4*, *5*). This prediction was supported by the fact that nonthermal radio emissions from Mercury had not been detected. Hence it appeared most probable that we would find no locally accelerated electron or proton fluxes in the 100-kev energy range associated with Mercury.

This is a preliminary report of our measurements from the Mariner 10 spacecraft, which show the presence at Mercury of large and impulsive fluxes of electrons with energies > 170 kev and protons with energies > 500 kev distributed over regions comparable in size to the planet itself. Our observations reveal physical conditions substantially different from those predicted for Mercury (*1*, *2*) based on the analogies mentioned above with other planets and the moon. The observed phenomena provide important clues for understanding the interaction of the solar wind with Mercury's magnetosphere which leads to the energizing of charged particles. We have benefited greatly in our interpretative work on the Mercury encounter of 29 March 1974 as a result of the exchanges of data with the magnetometer group (*6*) and the plasma science group (*7*) in the weeks preceding the preparation of this report. However, it is clear that a quantitative physical picture of the particle–magnetic field–plasma interactions will become possible only after an extensive collaboration of the three groups.

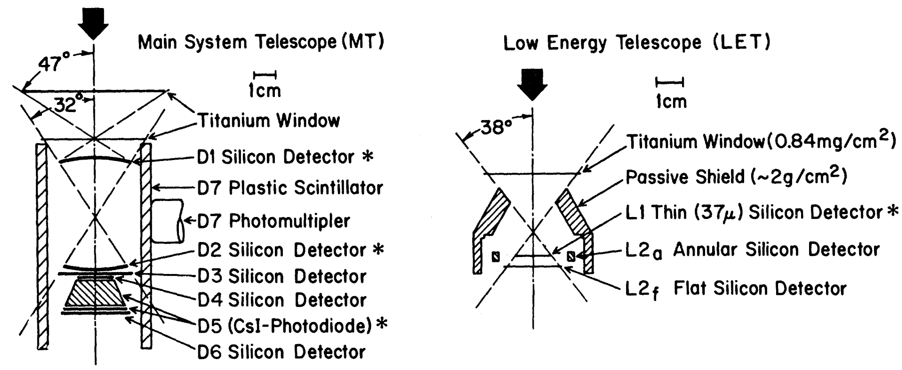

Fig. 1. Cross-sectional view of the University of Chicago charged particle telescopes. The view axes of the MT and the LET are parallel to within 5 degrees. This instrumentation is almost identical to the MT and LET onboard the Pioneer 10 and Pioneer 11 spacecraft (*10*).

Instrumentation. A general description of the University of Chicago instrument, its location on the Mariner 10 spacecraft, and the spacecraft trajectory has been published (*8, 9*). In the following discussion we have extended the description only to include those details essential for understanding our observations at Mercury. Cross-sectional views of the two charged particle telescopes in the instrument are shown in Fig. 1. Charged particles which enter the acceptance cones of these telescopes are identified as electrons, protons, and helium nuclei by both range of penetration in the detector stack and energy loss or residual energy deposited in those detectors (identified by an asterisk in Fig. 1) which have pulse height analyzers. Thus, the analysis of a given particle consists of the simultaneous output once each 0.33 second of the pulse height analysis and range information. The pulse height analysis operates in a statistical sampling mode for identification of particles during periods of large fluxes. The absolute fluxes are determined from the outputs of the counting rate accumulators, which count all particles satisfying the various range requirements. For instance, a particle entering detector D1 but not penetrating to detector D2 is called an ID1 event and is counted by the ID1 accumulator, whereas a particle entering detectors D1 and D2 but not detector D3 would be called a ID2 event and would be counted by the ID2 accumulator. There is a measurement of the accumulated number of events for each range interval every 0.6 second. From the known geometrical factors, the particle identification, and the counting rates we can determine the absolute fluxes and energy spectra of electrons and protons which are reported here. The rapid readout of the data was essential during the encounter in order to resolve the rapidly changing fluxes. For example, since the spacecraft velocity was $\sim$ 11 km sec^{-1}, the flux was measured in increments of $\sim$ 7 km (1/350 of the planetary radius) along the trajectory.

Our measurements at Mercury have shown that the energy ranges for electrons and protons were such as to restrict our measurements to detectors D1 and D2 in the main telescope and to the low energy telescope. The ID1 accumulator responds to protons and helium nuclei in the energy range 0.62 to 10.3 Mev per nucleon. It has an electron sensitivity which begins at an electron kinetic energy of approximately 170 kev. The experimentally determined efficiency, ε, for electron detection in ID1 is $\varepsilon = 8$ percent at 170 kev, 50 percent at 300 kev, and a maximum of 70 percent at 750 kev. The ID1 geometrical factor for electrons is approximately εG_e where $G_e = 14$ cm^2 sr; for protons $G_p = 7.4$ cm^2 sr.

The low energy telescope (LET) was designed to respond to 0.53- to 1.9-Mev protons, which trigger detector L1 but not L2 (designated as L1N2), and 1.9- to 8.9-Mev protons (designated as L12) without responding to electrons over a wide range of electron energies and intensities. To achieve this discrimination against electrons the L1 detector thickness was made $\sim$ 37 μm and the energy threshold for accepting pulses from L1 was set at 350 kev. Laboratory experiments have shown that the detection efficiency for low energy electrons for detector L1 is $\sim$ 1×10^{-5} (*10*). The dynamic range of the pulse height analyzer associated with detector L1 provides for the identification of protons and helium nuclei. A passive shield defines a geometrical factor of 0.49 cm^2 sr.

Experimental results. Before presenting the detailed analysis of our experimental results and their interpretation we have prepared in Fig. 2 a simplified overview of our measurements during the encounter, which places in perspective the time-intensity profiles of the locally accelerated energetic particles with respect to the main features of Mercury's magnetosphere (*6, 7*) and which relates all of these observations to the physical scale of the planet. To represent the particle measurements in Fig. 2 we choose the ID1 counting rate, which is the counting rate of electrons with a mean kinetic energy of $\sim$ 300 kev. We find four major features in the time-intensity profiles, which we designate as the A, B, C, and D events. The events are separated in time and space by flux levels which were close to the interplanetary background fluxes measured before and after encounter, as shown by the dashed line in Fig. 2. Since the Mariner 10 mission has occurred near solar minimum activity in the 11-year cycle, extensive periods of interplanetary quiet time (periods free from fluxes of particles accelerated in solar flares) exist throughout the mission, including the period of several days before, during, and after the Mercury encounter. We have reported the differential energy spectra for interplanetary electrons and protons under these conditions (*9*).

It is also important to emphasize the small scale of Mercury and its magnetosphere relative to the earth. The region over which the physical interactions occurred at Mercury is ~ 60 times smaller than the earth's magnetosphere for a similar trajectory. Hence, major magnetospheric features of global extent at Mercury are to be observed on time scales on the order of minutes along the Mariner 10 trajectory. The A, B, and C events are all within the magnetospheric boundaries of the planet, whereas the D event was observed in the magnetosheath on the outbound or "dawn side" pass. The asterisk at the intensity peak of the B and C events designates a period when the electron flux was so high that the ID1 counting rate became a nonlinear function of the true rate of incidence of electrons on D1; this is due to the electronic circuit response at these high counting rates (*10*).

In the following discussion we examine each of the four events in detail with respect to the kinds of particles present and their energy spectra, in order to decide whether the particles were trapped in the magnetic field of Mercury or whether they were transient phenomena.

The A event. We found no significant time-intensity structure in the A event for periods shorter than the 30-seconds used for the counting rate averages shown in Fig. 2. The electron flux increased by a factor of 10 over a distance of 1600 km from interplanetary background levels at the magnetospheric boundary. This was a region of generally increasing magnetic field intensity, with the field direction approximately radial from the planet (*6*) and within the view cones of both telescopes. The flux was ~ 99 percent electrons with a differential energy spectrum of $dJ_e/dE \propto E^{-3.0 \pm 0.5}$ derived from pulse heights corresponding to electrons of kinetic energy E from 200 to 600 kev. Less than 1 percent of the measured flux could be nucleons: the LET detected no flux of nucleons during this event.

The B event. At the onset of the B event shown in Fig. 3 the flux of ~ 300-kev electrons measured by the ID1 counting rate channel rose four orders of magnitude within 1.2 seconds, during which time the L1N2 counting rate channel, which measures the ~ 550-kev protons, remained at background level. Since the L1N2 and ID1 counting rate channels respond to protons of nearly the same energy, we conclude that the ID1 counting rate results only from electrons. Further, the lack of response of the LET during this time interval shows that the L1N2 counting rate channel has negligible electron sensitivity over the electron intensity range measured by the ID1 counting rate channel during this time interval. This immunity of the LET to electrons is in agreement with laboratory calibrations (*10*). The proton flux showed a similar abrupt increase at 2048:05 U.T. and returned to background at 2048:15 U.T. From the same arguments we also conclude that after the proton flux returned to background level, the remainder of the B event and B′ event (see Fig. 3) was due exclusively to electrons. We also found that at no time could the electron contamination of the L1N2 counting rate channel exceed 3 percent.

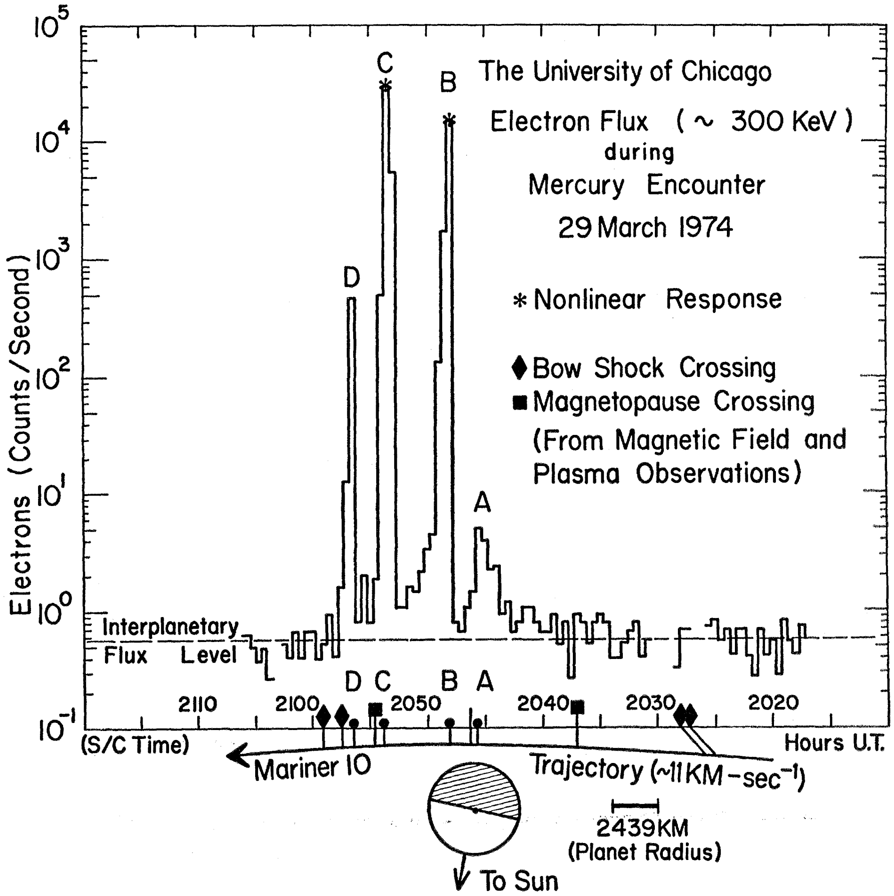

Fig. 2. Superposition of the ~ 300-kev electron counting rate and the main magnetospheric features (*6, 7*) projected onto the Mercury encounter trajectory of Mariner 10. Four charged particle events, A, B, C, and D, were observed. The position of maximum flux for each event is projected onto the trajectory. The trajectory is plotted in a plane defined by the centers of the sun, Mercury, and the spacecraft, with the sun-Mercury line held fixed.

Whenever the true flux leads to a counting rate in ID1 or L1N2 above ~ 3×10^4 counts per second, the electronics respond nonlinearly to the higher flux levels (*10*). Although the absolute counting rate is not directly determined above ~ 3×10^4 counts per second, approximate values for the true counting rate can be deduced from the observed counting rate by using experimentally determined conversion factors (*10*). The counting rates for the ~ 550-kev protons never reach the nonlinear region. However, the fluxes of ~ 300-kev electrons in both the B and C events (see Fig. 4) were in this region for approximately 10 seconds. These periods are identified in Figs. 3 and 4 by the "flat-tops" on the observed counting rates at ~ 5.5 $\times 10^4$ counts per second. The true counting rates at these times were higher by a factor of 10 to 20 than the indicated values shown in Figs. 3 and 4.

In addition to the evidence presented above that the LET was measuring protons and the ID1 was measuring electrons in the B event, we have examined the question whether these detector systems could be responding to a pulse pile-up effect from electrons with energies below the ID1 electron threshold, under the assumption that the flux of lower energy electrons would continue to rise steeply below this threshold energy. We found from a study of the rate of change of the ID1 and L1N2 counting rates and the experimentally determined L1 electron efficiency that such an assumption of subthreshold energy electron pileup is inconsistent with the data.

We also note that the simultaneous observations of approximately equal proton and electron fluxes such as observed at 2048:05.2 U.T. proves that there can be no substantial spacecraft charge contributing to local acceleration of the protons or electrons which we measure.

If the differential energy spectrum for protons is represented as $dJ_p/dE \propto E^{-\gamma_p}$ then we find $5 \leq \gamma_p \leq 7$ as the range for γ_p in the B event. Both counting rate data from L1N2 and L12 and pulse height distributions lead to this conclusion. The energy spectrum of the protons measured by the LET implies that the ID1 flux was always dominated by electrons. The electron energy spectrum in the B event is difficult to determine because the flux decreases extremely rapidly with increasing energy. The ID1 pulse height analysis and the fact that no electrons are observed to penetrate to detector D2 set a limit of $\gamma_e \geq 9$ for an assumed spectral form of $dJ_e/dE \propto E^{-\gamma_e}$ for $E > 170$ kev.

The magnetic field intensity decreased rapidly in coincidence with the onsets of both the B event and the B′ event and then increased rapidly (*6*). The direction of the magnetic field in the B event was such that for electrons and protons to enter the cone angle of acceptance of the telescopes they must have pitch angles with respect to the magnetic field of $\gtrsim 20$ degrees and ≥ 40 degrees, respectively. The electron detector in the plasma instrument observed an enhanced electron flux, beginning with the onsets of the B and C events (*7*).

The B event provided sufficient information for us to decide whether the particle fluxes are stably trapped or are transient. The spacecraft velocity was ~ 11 km sec^{-1}, and for a stable trapping region the spacecraft would require 4 seconds to move one electron gyroradius in the magnetic field of 5×10^{-4} gauss which was typical of that region. Since the gyroradius of the protons is ~ 2100 km, the time to move one proton gyroradius would be ~ 200 seconds. However, from

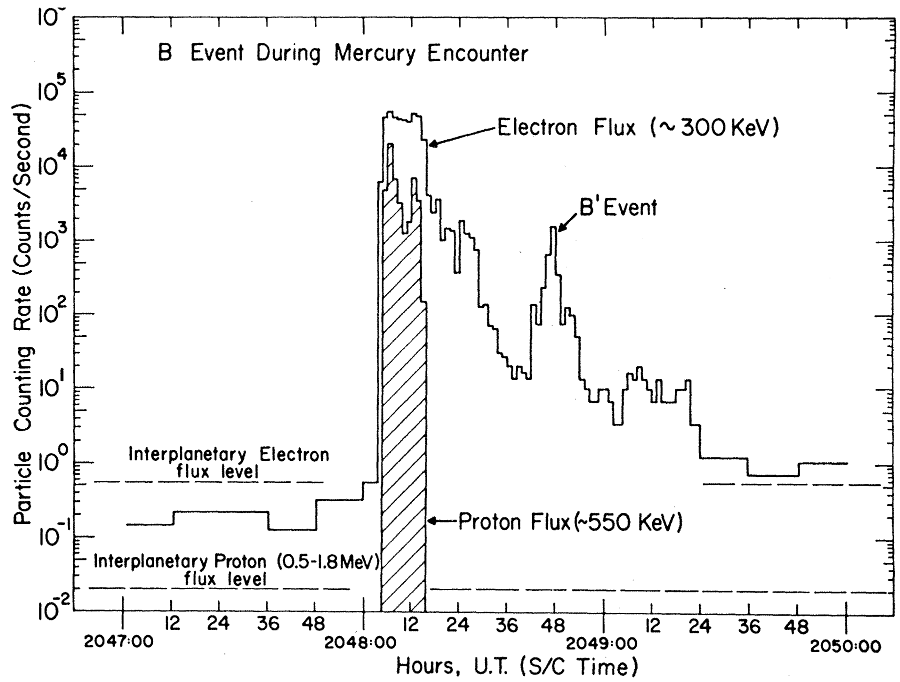

Fig. 3. The B event counting rates of $\sim$ 300-kev electrons and $\sim$ 550-kev protons. Tick marks on the abscissa represent 12-second intervals. The counting rates are averaged over 1.2 seconds whenever they are significantly above 1 count per second. Note that $\sim$ 6 seconds separate the two proton peaks and that the three peaks in the B′ event are also separated by $\sim$ 6 seconds.

Fig. 3 it is clear that the flux increase of both electrons and protons occurred within $\sim$ 2.5 seconds. Therefore the fluxes are either transient effects or represent particles transported by the magnetic field past the spacecraft at high velocity to simulate a rapid onset and rapid intensity variations. Although the magnetic field did switch direction near the onset of the B event, it returned to its pre-onset direction within $\sim$ 1 second (*6*). There was no subsequent correlation of magnetic field directional variations with particle intensity variations. We consider this evidence that the particle fluxes observed in the B event (and later in the C event) were transient phenomena.

Additional evidence that the events are impulsive may be derived from the B event, namely, that the duration of the enhanced proton fluxes in the B event is only 12 seconds, corresponding to a spatial extent of only $\sim 1/16$ of the proton gyroradius. Furthermore, since the spacecraft was only about 1200 km or about 0.5 of a proton gyroradius above Mercury's surface during the B event, we see that the protons in this event must have been captured by the planet.

The small upper limit set by dispersion of $\sim$ 1.2 seconds between the onsets of the electron and proton fluxes is also important to note since the velocity ratio $V_e/V_p \gtrsim 30$. This is strong evidence that the particles, if produced simultaneously in an impulsive event, have not traveled great distances before detection.

The C event. Between the end of the B event and the onset of the C event shown in Fig. 4, the electron and proton fluxes were at interplanetary levels for approximately 3.5 minutes. The initial rate of increase of the electron flux was slower than for the B event by a factor of approximately 3; that is, there was an increase of $\sim 10^4$ in electron flux in 4 seconds. The arguments applied to the B event to show that the ID1 counting rate channel was measuring the electron flux and that the L1N2 channel was measuring the low energy proton flux are found to hold for the C event. In addition, similar arguments can be invoked to show that the L12 channel was measuring protons for event C.

In Fig. 4 it is clear that there is an approximately 6-second periodicity in the electron and proton counting rates. From a power spectrum analysis (*11*) of the electron intensity variations from 2052.57 to 2053:24 U.T. we obtained a characteristic period of 6.6 ± 1.2 seconds and higher frequency components, while in the interval 2053:36 to 2054:12 we obtained a strong peak at

~ 10 seconds in addition to the one at 6.6 ± 1.2 seconds and the higher frequency components. We have made a detailed study of these periods to decide whether they could have been artifacts arising from spacecraft noise, instrument malfunction, or noise introduced in the data system. We conclude that the oscillations or "ringing effects" are variations of particle intensity and may reflect the dynamics of the energizing process, which we shall discuss later. Although the magnetic field shows considerable structure in intensity and direction during the C event, no readily apparent magnetic field signature was noted which could be considered coincident with any particle intensity change except that the flux level in the C event terminated abruptly by dropping three orders of magnitude at the magnetospheric boundary (*6, 7*). Since the mean magnetic field was approximately 5×10^{-4} gauss during the C event, if we were to interpret the 6-second periodic variation as a spatial feature it would correspond to twice the electron gyroradius and 1/30 of the proton gyroradius. This is independent evidence that the electron and proton fluxes are transient phenomena.

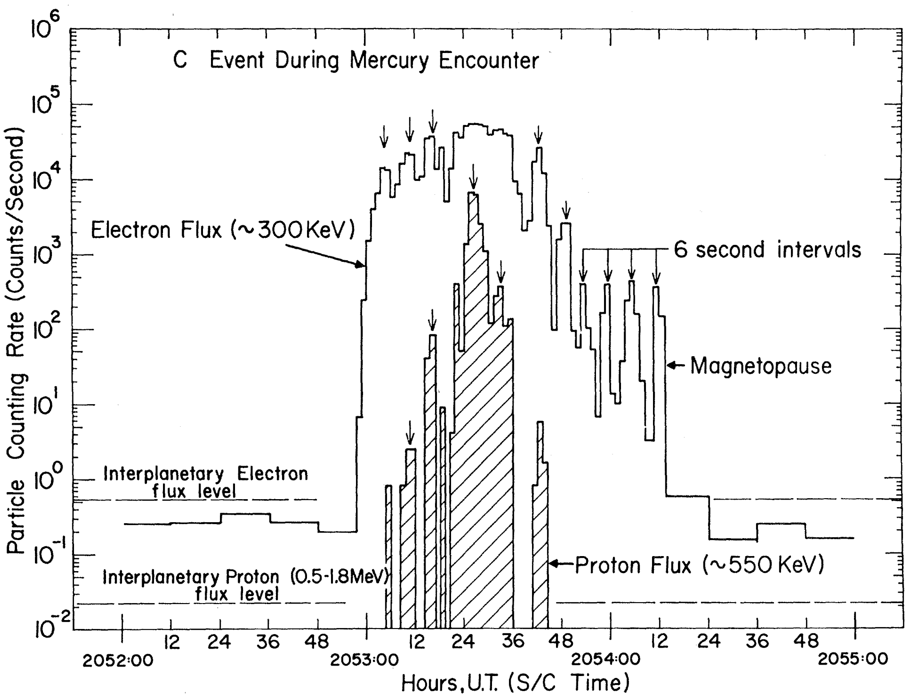

Fig. 4. The C event counting rates of ~ 300-kev electrons and ~ 550-kev protons averaged over 1.2-second intervals. These fluxes exhibit a periodicity of ~ 6 seconds and terminate at the magnetopause (*6, 7*).

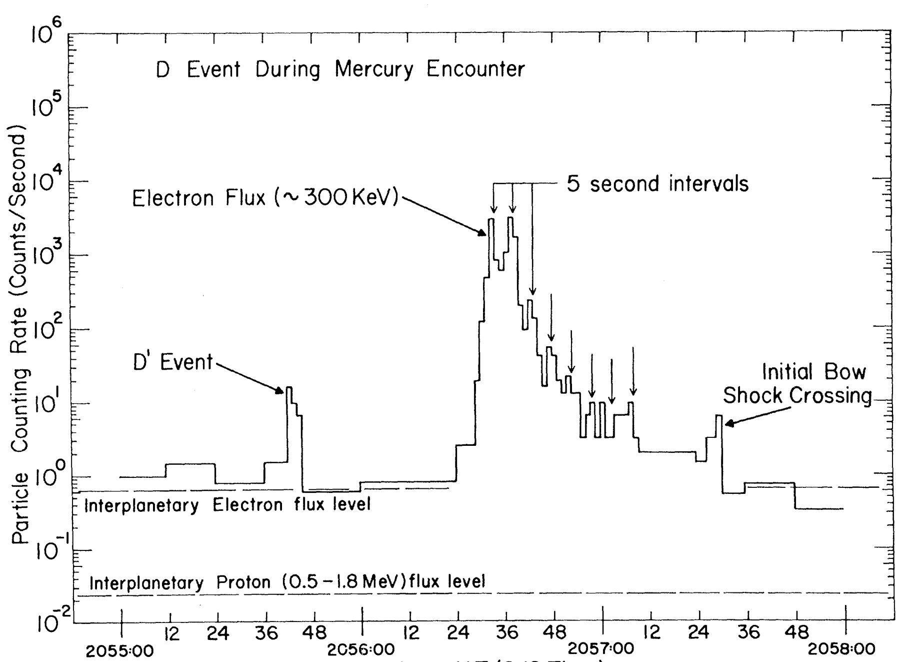

Fig. 5. The D event counting rates of ~ 300-kev electrons. Both the D′ event and the D event occurred within the magnetosheath. Note the marked 5.0-second periodicity of the D event. The bow shock crossing was identified by magnetic field (*6*) and plasma (*7*) observations.

The D event. The electron flux as measured by the ID1 counting rate channel was at interplanetary levels during passage through the magnetosheath except for the D′ and D events as shown in Fig. 5. Throughout the magnetosheath crossing and bow shock crossings the ~ 550-kev proton flux remained at the interplanetary level which existed before encounter and which persisted beyond the bow shock after encounter. The electron pulse height distribution for the D event was similar to that for the B and C events: namely, for an assumed power law spectrum, $\gamma_e \geqq 9$. No additional electron flux increases were observed in the successive bow shock crossings (*6, 7*) which arose from the motion of the bow shock across the spacecraft. We note that the intensity increase was ~ 10^3 in 2.4 seconds and that the oscillations of electron intensity displayed an approximately 5-second period for at least eight periods.

We analyzed this oscillation by using the method of Blackman and Tukey (*11*) to obtain the power spectrum of the spectral density versus frequency displayed in Fig. 6. The maxima are at 0.20, 0.40, and 0.66 hertz. These frequencies (ν) correspond to periods of 5.0 ± 1.0, 2.5 ± 0.3, and 1.5 ± 0.1 seconds. In Fig. 6 we note that the maxima are modulated by an intensity dependence which is proportional to $\exp(-a\nu)$, where a is a constant.

In contrast with the B and C events, where no correlation between electron and magnetic field intensity variations were observed, we found that the D event intensity variations were strongly correlated with oscillatory changes in direction of the magnetic field. The electron intensity maxima occurred when the magnetic field was approximately southward and solar in direction, whereas the intensity minima occurred when the field was approximately northward and antisolar in direction (*6*).

Discussion and conclusions. So far in this report we have presented only the experimental facts obtained by direct analysis of the data. We now examine their interpretation in terms of alternate models for acceleration and propagation of the electrons and protons to demonstrate that the unique character of the phenomena discovered in Mercury's magnetosphere eliminate some magnetospheric acceleration hypotheses and place strong constraints on others.

The first question to settle is whether the radiation is primarily trapped (that is, whether there is a spatial distribution of fluxes) in the magnetic field, or is transient radiation. If the radiation is transient, we want to know whether the accelerating region is continuously feeding particles to the field lines on which the observations are made, or is impulsively injecting the particles. We first consider the events within Mercury's magnetospheric boundary. No unambiguous answer to these questions can be obtained from the A event, which could, for example, correspond to a trapped electron population, especially if the dipole model for the magnetic field suggested by Ness *et al.* (*6*) is confirmed. Such a population would be rapidly depleted by gradient drifts in the magnetic field, the depletion being dependent on the magnetic field geometry or the source of the electrons. Two possible sources for these electrons are a remnant flux from an impulsive event like the B event, or radioactivity from the planet's surface. However, our observations of the B and C events enable us to choose among the above alternatives. Namely, we conclude that

1) The transitory nature of both the electron and proton fluxes is not due to the magnetic field carrying these particles swiftly past the spacecraft to simulate rapid intensity variations.

2) The B event occurred when the distance of the spacecraft to the planet's surface was less than the proton gyroradius in the observed magnetic field. Therefore the observed protons must be captured by the planet. Thus, if Mercury has an atmosphere this radiation may produce aurora-like effects.

3) The duration of the enhanced proton fluxes in the B and C events is only ~ 2 to 15 seconds. This corresponds to a spatial extent of less than 0.1 of the proton gyroradius in the measured magnetic field. Consequently these protons must be bursts and cannot be part of the stably trapped population.

4) The approximate 6-second oscillations observed for both events are not due to periodic changes in the magnetic field geometry or intensity. The periodicity and near simultaneous observations of both electron and proton fluxes require that the particles of opposite electric charge are accelerated in the source at, or near, the same time. It appears that the oscillations are to be associated with the source mechanism.

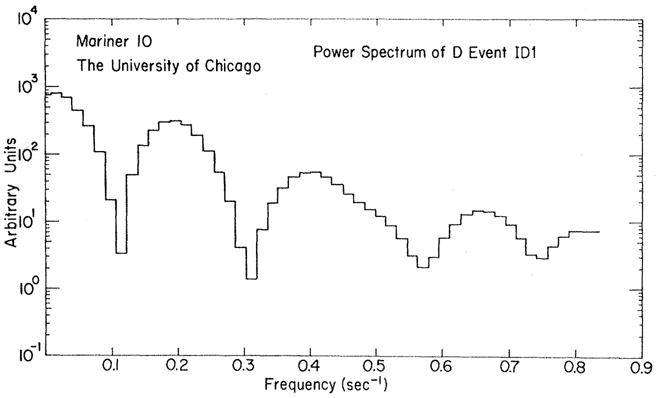

Fig. 6. Power spectrum of the ~ 300-kev electron counting rate during the D event. The fundamental frequency response is at 0.2 hertz with higher frequency components at 0.4 and 0.66 hertz. If the periodicity in the D event were not coherent, the frequency response would average out to a straight line.

Since the electrons and protons in the B and C events have such strikingly similar characteristics—including their energy spectra—we are led to the conclusion that they are both manifestations of the same kind of acceleration mechanism. Furthermore the high intensity electron and proton events observed inside the magnetosphere are transient events and are not interpretable as spatially distributed trapped particle populations.

We can estimate the distance that particles travel along the magnetic field lines between the point of impulsive acceleration and the point of observation if we make the assumption that both protons and electrons are accelerated to their observed energies simultaneously. Since the ratio of particle velocities along the magnetic field line is $V_p/V_e \cong 0.03$ and the difference in observed rise times is 1 to 2 seconds for the burst events, we see that the source could not be more than $\sim 8 \times 10^3$ km ($\sim 3\ R_M$, where R_M is the planetary radius) for the B event and less than 16×10^3 km ($\sim 6.5\ R_M$) for the C event. Since the proton cyclotron period in the observed magnetic field is itself ~ 1 second we see that the above values derived from time dispersion must be upper limits.

Before discussing possible acceleration mechanisms, we compare the D event to the B and C events. The D event occurred within the magnetosheath before the first outbound crossing. The electron intensity shows a marked periodicity of 5 seconds, comparable to the 6-second periodicity observed in the B and C events, but was much more coherent, as demonstrated in Fig. 6. Otherwise, except for intensity, we conclude that the D event is similar in characteristics to the B and C events.

The most likely candidates for the magnetospheric regions in which the impulsive acceleration could occur are either the region between the bow shock and the magnetopause, or the magnetotail extending behind the planet between magnetospheric boundaries.

The features of the D event could possibly be explained by assuming particle acceleration in the magnetosheath associated with the moving bow shock. The absence of protons in this event may be due to the large proton gyroradius relative to the distance between the bow shock and the magnetospheric boundary. A strong correlation of the magnetic field variations with the ~ 5-second periodic electron intensity variation leaves open the question of whether the electron flux is being modulated by the local magnetic field changes, or whether the oscillation is to be associated with the acceleration region. On the other hand, if the magnetosheath were the only region for particle acceleration at Mercury it would be difficult to account for the appearance of both electrons and protons far inside the magnetospheric boundary where the B and C events were observed, and at the same time preserve their persistent ~ 6-second periodicity and very sharp rise times.

Alternatively, impulsive acceleration of electrons and protons in the magnetotail of the planet is an attractive possibility since it can account for the major features of the B and C events. There are several analogies which can be made with the phenomena observed in the earth's magnetotail, such as the so-called substorm effect in which electrons and protons are accelerated as a result of a sudden instability occurring in the magnetic tail region.

The phenomena we discovered at Mercury, however, place more stringent conditions on allowed models for impulsive acceleration than have heretofore been possible in studies of the earth's magnetosphere. For example, the rise times for each proton burst—and therefore the time limit for energizing protons to $\gtrsim 0.5$ Mev—is less than the time required for a proton to undergo one cyclotron period in the magnetic field (which we have assumed to be $\sim 5 \times 10^{-4}$ gauss). Therefore, no theories or models for magnetic field interactions involving many cyclotron periods can be operative. The consequence of this conclusion is that models invoking strong, impulsive electric fields appear to be required for the simultaneous acceleration of protons and electrons. For example, ion–acoustic wave acceleration (*12*) and even slow neutral sheet merging of magnetic fields may not account for the observations. The question of whether phenomena such as fast neutral sheet merging, sheet pinch instabilities (*13*), or runaway processes (*14*) can account for the postulated impulsive acceleration remains to be explored later.

The periodic oscillation of the electron intensity in the B and C events without accompanying periodic variations in the local magnetic field points strongly to the acceleration region as the source of the oscillation or "ringing effect." Indeed, this is fully supported by the series of impulsive proton bursts accompanying electron oscillations in the C event (Fig. 4). This effect will undoubtedly place strong constraints on models to be developed for explaining the impulsive acceleration of the particles.

Mercury's magnetosphere can provide sufficient energy for the observed bursts of electron and proton fluxes. We find that the maximum rate of energy input required to accelerate the protons and electrons we observed in the B event is $< 10^{-2}$ of the rate of energy input of the solar wind into the magnetosphere. Therefore the mechanism of acceleration must also be very efficient. Since the energy spectra of the protons and electrons undoubtedly extend to lower energies and higher flux levels below our observational thresholds, it is quite clear that although there is sufficient energy via the solar wind–magnetic field–charged particle interactions, the energy spectra of protons and electrons must turn over below the detection thresholds in our experiment in order not to exceed the magnetic field energy density.

Clearly, a second encounter of Mariner 10 with Mercury through the magnetotail region of the planet would be of major importance for resolving the remaining questions on impulsive acceleration of Mercury's electron and proton fluxes.

J. A. SIMPSON, J. H. ERAKER
J. E. LAMPORT, P. H. WALPOLE
Enrico Fermi Institute, University of Chicago, Chicago, Illinois 60637

References and Notes

1. S. J. Bame, H. S. Bridge, L. A. Frank, J. W. Freeman, K. W. Ogilvie, C. W. Snyder, J. H. Wolfe, C. M. Yeates, "Final report of the plasma instrument team for the 1973 Mercury/Venus mission design study," preprint.
2. J. A. Simpson, S. M. Krimigis, J. E. Lamport, C. O. Bostrom, J. W. Kohl, W. T. Huntress, Jr., *JPL Document 615-5* (Jet Propulsion Laboratory, Pasadena, Calif., 1970).
3. P. Goldreich and S. J. Peale, *Astron. J.* **71**, 425 (1966).
4. N. F. Ness and Y. C. Whang, *J. Geophys. Res.* **76**, 1316 (1971).
5. F. C. Michel, *Comments Astrophys. Space Sci.* **3**, 27 (1971).
6. N. F. Ness, K. W. Behannon, R. P. Lepping, Y. C. Whang, K. H. Schatten, *Science* **185**, 151 (1974).
7. K. W. Ogilvie *et al.*, *ibid.*, p. 145.
8. J. A. Dunne, *ibid.* **183**, 1289 (1974); *ibid.* **185**, 141 (1974).
9. J. A. Simpson, J. H. Eraker, J. E. Lamport, P. H. Walpole, *ibid.* **183**, 1318 (1974).
10. J. A. Simpson, D. C. Hamilton, R. B. McKibben, A. Mogro-Campero, K. R. Pyle, A. J. Tuzzolino, *J. Geophys. Res.*, in press.
11. R. B. Blackman and J. W. Tukey, *The Measurement of Power Spectra* (Dover, New York, 1958).
12. F. L. Scarf, W. Bernstein, R. W. Fredricks, *J. Geophys. Res* **70**, 9 (1965); R. W. Fredricks, F. L. Scarf, W. Bernstein, *ibid.*, p. 21.
13. B. Coppi, G. Laval, R. Pellet, *Phys. Rev. Lett.* **16**, 1207 (1966).
14. M. J. Houghton, preprint.
15. We wish to acknowledge the support of many individuals and groups which made these experiments possible. At the University of Chicago the instrument was designed and built in the Laboratory for Astrophysics and Space Research of the Enrico Fermi Institute and the preparation of programs and preliminary analysis were undertaken by G. Lentz, J. Coates, S. Christon, S. Daly, and A. J. Tuzzolino. The laboratory electron calibrations were carried out with the assistance of R. Zamow. We thank E. N. Parker for a valuable discussion of our results. At the Jet Propulsion Laboratory we are especially grateful for the support of W. Giberson, J. Dunne, A. Matzke, D. Swenson, and J. Tupman. It is clear that this mission could not have been successful without the strong support of J. E. Naugle, N. W. Cunningham, and S. E. Dwornik at NASA Headquarters. This research was supported in part by JPL contract 953091, NASA grant NGL 14-001-006, and NSF grant GA-38913X.

14 June 1974

Mercury's Atmosphere from Mariner 10: Preliminary Results

Abstract. *Analysis of data obtained by the ultraviolet experiment on Mariner 10 indicates that Mercury is surrounded by a thin atmosphere consisting in part of helium. The partial pressure of helium at the terminator is about 5×10^{-12} millibar. The total surface pressure of the atmosphere is less than about 2×10^{-9} millibar. Upper limits are set for the abundance of various gases, including hydrogen, oxygen, carbon, argon, neon, and xenon. The wavelength dependence of Mercury's surface albedo is similar to that of the moon over a broad range of wavelengths from 500 to 1600 angstroms. Strong signals were recorded by the airglow instrument as Mariner 10 passed through the cavity behind Mercury. They are as yet unexplained but may provide information on the properties of the local plasma.*

Two instruments sensitive in the extreme ultraviolet were carried aboard Mariner 10: an occultation spectrometer to measure the extinction properties of the atmosphere as the sun is occulted by the limbs of the planet, and a spectrometer to search for airglow at wavelengths elected to identify specific atmospheric gases. The airglow instrument has previously observed constituents in the upper atmospheres of the earth and Venus (*1*).

We concentrated attention on noble gases such as He, Ar, and Ne, since there are several obvious supply processes for these gases. Helium and neon can be captured from the solar wind; helium and argon may be released by decay of radioactive elements in Mercury's crustal rocks. A preliminary examination of the mass balance for the various species on Mercury leads us to conclude that the most probable species would be Ar, Ne, and He. The choice of airglow channels reflects this analysis. However, the instrument was also designed to detect emissions associated with H, O, and C.